ACS Chemical Neuroscience

pubs.acs.org/chemneuro Research Article

Binding Modes and Selectivity of Cannabinoid 1 (CB1) and Cannabinoid 2 (CB2) Receptor Ligands

Jing-Fang Yang, Alexander H. Williams, Narsimha R. Penthala, Paul L. Prather, Peter A. Crooks, and Chang-Guo Zhan*

Cite This: https://dx.doi.org/10.1021/acschemneuro.0c00551 Read Online

ACCESS | Metrics & More | Article Recommendations | Supporting Information

ABSTRACT: The cannabinoid (CB) receptors (CB_1R and CB_2R) represent a promising therapeutic target for several indications such as nociception and obesity. The ligands with nonselectivity can be traced to the high similarity in the binding sites of both cannabinoid receptors. Therefore, the need for selectivity, potency, and G-protein coupling bias has further complicated the design of desired compounds. The bias of currently studied cannabinoid agonists is seldom investigated, and agonists that do exhibit bias are typically nonselective. However, certain long-chain endocannabinoids represent a class of selective and potent CB_1R agonists. The binding mode for this class of compounds has remained elusive, limiting the implementation of its binding features to currently studied agonists. Hence, in the present study, the binding poses for these long-chain cannabinoids, along with other interesting ligands, with the receptors have been determined, by using a combination of molecular docking and molecular dynamics (MD) simulations along with molecular mechanics-Poisson−Boltzmann surface area (MM-PBSA) binding free energy calculations. The binding poses for the long-chain cannabinoids implicate that a site surrounded by the transmembrane (TM)2, TM7, and extracellular loop (ECL)2 is vital for providing the long-chain ligands with the selectivity for CB_1R, especially I267 of CB_1R (corresponding to L182 of CB_2R). Based on the obtained binding modes, the calculated relative binding free energies and selectivity are all in good agreement with the corresponding experimental data, suggesting that the determined binding poses are reasonable. The computational strategy used in this study may also prove fruitful in applications with other GPCRs or membrane-bound proteins.

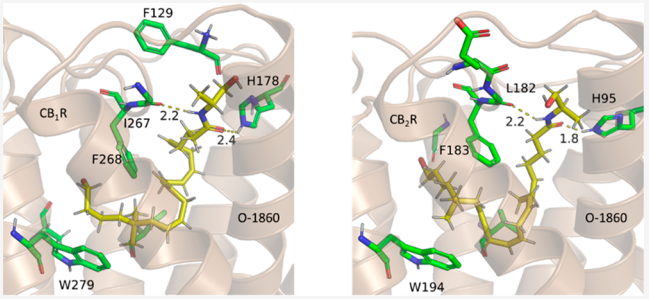

KEYWORDS: *Cannabinoid receptor, selectivity, endocannabinoid, drug design strategy, modeling*

Downloaded via CARLETON UNIV on October 4, 2020 at 12:17:13 (UTC).
See https://pubs.acs.org/sharingguidelines for options on how to legitimately share published articles.

INTRODUCTION

G-protein coupled receptors (GPCRs) are a well-studied class of proteins, with significant viability as therapeutic targets due to their functions in critical physiological pathways.[1] Currently, there are over 400 approved drugs targeting these receptors, with over 100 targets represented among them.[1] The cannabinoid (CB) receptors are a subset of the GPCRs, consisting of seven transmembrane (TM) regions divided into two subtypes: CB1 receptor (CB_1R) and CB2 receptor (CB_2R). Each of these subtypes has characteristic functions related to their distribution in the body. While both CB_1R and CB_2R are found within the brain, CB_2R is additionally expressed in the periphery, most prominently within the spleen.[2] These receptors' primary function within the body is the regulation of adenylyl cyclase, which is implicated in nociception.[3−6] This implication has led to a levy of studies performed to determine the cannabinoids' abilities to produce analgesic effects as a potential replacement for nonsteroidal anti-inflammatory drugs (NSAIDs) and opioids, which both come with a set of noxious side effects.[4,5,7−14] Additionally, the knockout (KO) of CB_1R has been implicated in the protection against obesity due to the CB receptors' functions in regulating metabolism.[15] These relationships have made the CB receptors a promising target for several therapeutic indications. However, there has yet to be a U.S. Food and Drug Administration (FDA)-approved selective cannabinoid agonist for either CB_1R or CB_2R, an advantageous property that would allow for the limiting of off target effects induced by these previously approved nonselective therapeutics.[16,17]

Current drug design targeting CB_1R or CB_2R primarily falls within the small-molecule space, with the molecules studied utilizing the same binding site as the phytocannabinoid class, *e.g.*, (−)-*trans*-Δ^9-tetrahydrocannabinol (THC), cannabidiol (CBD), and cannabigerol (CBG).[18] This binding site has been studied extensively and has previously had several star

Received: August 21, 2020
Accepted: September 18, 2020

ACS Publications © XXXX American Chemical Society

compounds (*e.g.*, rimonabant and WIN-55,212) tailored to it.[19−22] While the cannabinoid agonists targeting this site can exhibit high potency toward the CB receptors, many are ultimately unable to exhibit high selectivity toward either receptor.[23,24] Interestingly, the endogenous cannabinoids (endocannabinoids) with a long carbon chain structural scaffold (Figure 1) exhibit considerable selectivity toward

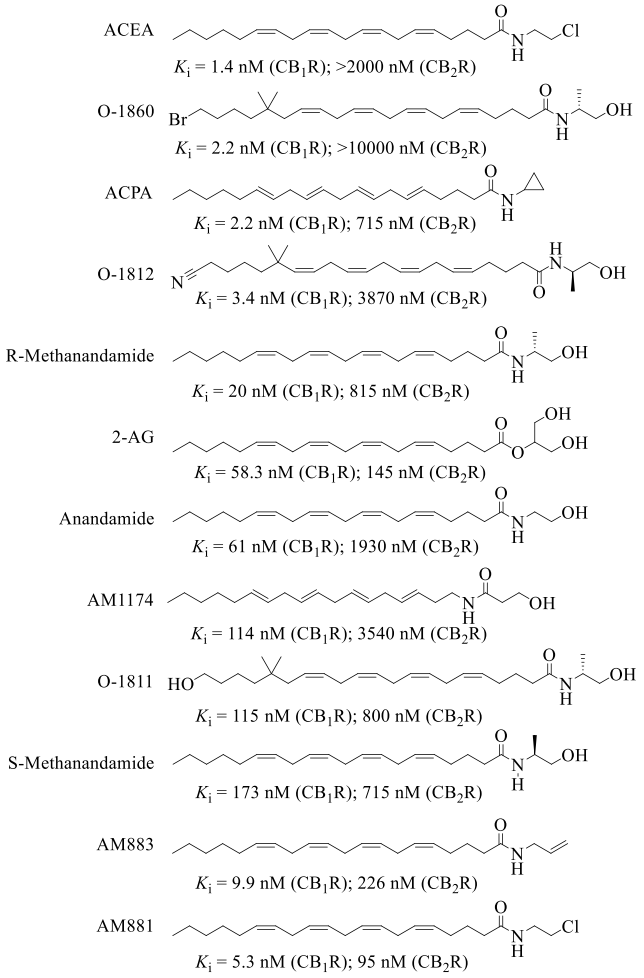

Figure 1. Representative long-chain endocannabinoids and their synthetic analogues. The experimental binding affinities come from the references indicated in Table 2.

CB_1R, with comparable potency to many of these previously reported compounds.[18,25,26] With minimal modifications to these endogenous ligands, analogues of these endocannabinoids exhibit greater selectivity and potency than their precursors (Figure 1).[27] However, these long-chain ligands have been far less studied concerning their potential as CB receptor agonist therapeutics in comparison to compounds with structural similarity to the phytocannabinoids. The indole quinuclidinone (IQD) compounds, PNR-4-20 and PNR-4-02, were the only reported G-protein biased agonists of CB_2R (Figure 2).[28] Incorporating the binding modes of these long-chain endocannabinoids with the recently published new agonists, including a G-protein biased agonist, could be a viable path toward the rational design of the desirable CB_1R-specific and G-protein biased agonists.[29−33] Hence, it is crucial for rational design of CB_1R-specific ligands to first determine how these compounds (Figure 1 and 2) bind with both CB_1R and CB_2R and to understand the nature of their selectivity.

There have been various reports of computational and experimental studies on CB_1R and CB_2R binding with various ligands. Reported cryogenic electron microscopy (Cryo-EM) structures of CB_1R or CB_2R binding with ligands revealed a commonly available binding site, *i.e.*, the phytocannabinoid binding site, for a few ligands examined so far.[21,22,34−37] Previously reported computational studies have been focused on the phytocannabinoid binding site.[19,20,22,38−40] None of the previously reported computational studies examined the possible binding poses of the IQD series of compounds (Figure 2), and there have been few reports concerning the binding poses of the long-chain endocannabinoids.[19,20,22]

Particularly, studies concerning the long-chain endocannabinoids and their analogues have primarily been *in vitro* based, using structure−activity relationships (SARs) to discover productive modification for these agonists.[25,27,41−43] Through these studies, several important factors have been determined such as the necessary aliphatic chain length for CB_1R binding, and the importance of double bonds within the aliphatic chain.[41] Previous *in silico* attempts at explaining the binding mode of these compounds have relied on homology-based methods of the cannabinoid receptors which were inaccurate in comparison to the recently published structures.[44] One attempt to elucidate the binding mode of these endocannabinoids came from McAllister et al. which proposed a folded anandamide structure within a homology-modeled CB_1R.[44] A similar binding mode was also reported by other groups using molecular docking to homology-modeled CB_1R.[37] However, the recently published Cryo-EM structures of CB_1R and CB_2R revealed that the phytocannabinoid binding sites within these receptors possess significant similarity within the pocket proposed for anandamide, eliminating the possibility for CB_1R selectivity.[21,22,35,36] These new Cryo-EM studies also attempted to computationally place long-chain cannabinoids within the resolved structures of CB_1R. While these binding poses were stable when subjected to short-time scale molecular dynamics (MD) simulations, they did not comment on the selectivity of these compounds; additionally, their proposed binding modes for these compounds at CB_1R relied heavily on the central channel binding pocket, thus lacking any major differences between the two receptors that could be used to determine their selectivity for CB_1R.[21,22] With this similarity of the central binding pocket in mind, it is critical to explore possible binding modes for these endocannabinoids that do not solely rely on the typical phytocannabinoid binding pocket to decide their selectivity.

Recent advancement in computational power and support for GPU-accelerated hardware have made long-time scale MD simulations (0.1−1 μs) more feasible for large-scale systems, including lipid bilayers with proteins embedded within them.[45] Through a combination of the MD simulations and molecular mechanics−Poisson−Boltzmann surface area (MM-PBSA) binding free energy calculations, compounds binding with a given protein can be ranked accurately in correlation with their experimental binding free energy (ΔG_{exp}) values.[45,46] Our group has previously been successful in developing and utilizing various computational approaches for modeling ligands binding with the transmembrane proteins to elucidate subtype selectivity.[47−51] Hence, in the present study, we employed a variety of computational methods, including molecular docking, MD, and MM-PBSA, to explore the

https://dx.doi.org/10.1021/acschemneuro.0c00551
ACS Chem. Neurosci. XXXX, XXX, XXX−XXX

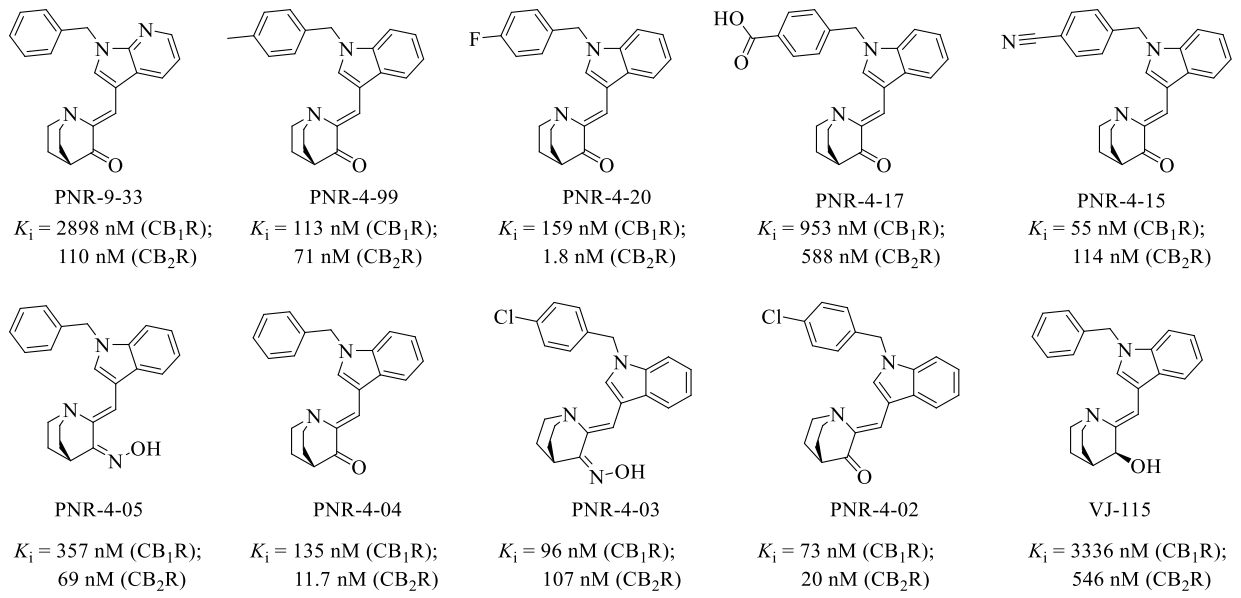

Figure 2. Molecular structures of indole quinuclidinone (IQD) series cannabinoid receptor agonists, along with the experimental binding affinities.[28]

binding poses of these interesting compounds (Figures 1 and 2) with CB_1R and CB_2R and reveal the binding and selective mechanism. According to the computational data, the IQD series of compounds bind to the receptors in the known traditional binding site (phytocannabinoid binding site) of the receptors, whereas the long-chain cannabinoids bind to the receptors in a binding mode which is more favorable for CB_1R. These computationally determined binding modes show excellent correlation with the empirically obtained binding data, suggesting that these binding modes are reasonable for these receptors.

RESULTS AND DISCUSSION

Due to the high binding selectivity and potency of O-1860 with CB_1R, its binding mode was studied closely, in the present study, to determine potential unique binding features through molecular docking and MD simulations (Figure 3A and 3B). The obtained binding mode of O-1860 reveal a previously unused binding site in proximity to the extracellular interface of the receptor. As opposed to the previously suggested binding modes concerning these compounds, the hydrophilic binding site within the extracellular interface of CB_1R provides pivotal interactions with the long-chain endocannabinoids. Within this region, there are additional critical residue substitutions within CB_2R that change the binding pocket's ability to receive these long chain endocannabinoids. The critical change between the two receptors is from a change in I267 in CB_1R to L182 in CB_2R (Figure S1 in the Supporting Information). This change causes a steric clash with the long-chain cannabinoids (Figures S3–S14), increasing the hydrogen bond-related distance with L182 and the ligand (Figure 3B) and reducing van der Waals (vdW) interactions with the receptor (Table 1). Conversely, the stricter binding site from these residues in the extracellular interface creates a method to induce CB_1Rselectivity. The size of the agonist supported by the binding pocket in CB_2R will be decreased due to these residue changes from CB_1R to CB_2R. From these initial results concerning the binding free energy of O-1860, one can see the large differences in the experimental binding affinity be

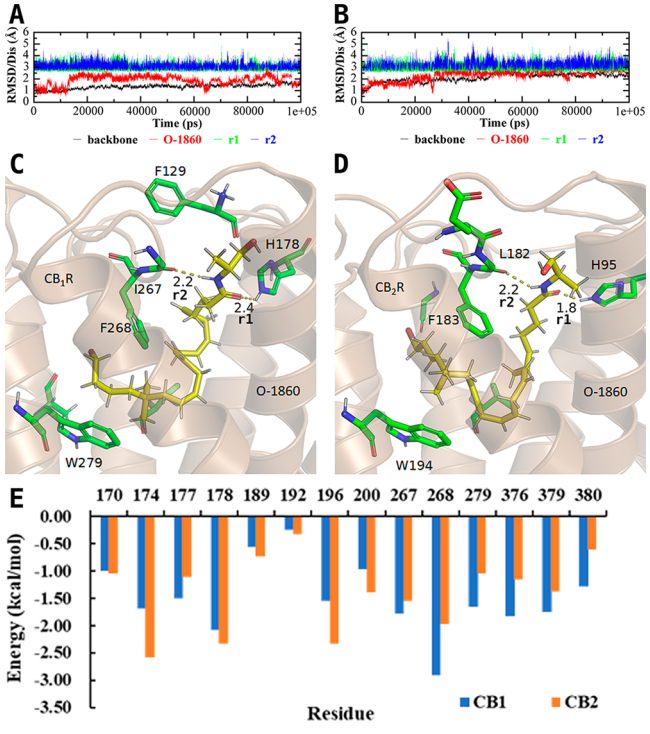

Figure 3. (A) Room-mean-square deviation (RMSD) of backbone atoms (black) of CB_1R and heavy atoms of O-1860 (red) along with two crucial distances (r1 and r2) indicated in panel (C) in the MD-simulated CB_1R binding with O-1860. (B) RMSD of backbone atoms (black) of CB_2R and heavy atoms of O-1860 (red) along with two crucial distances (r1 and r2) indicated in panel (D) in the MD-simulated CB_2R binding with O-1860. (C) Snapshot of the MD-simulated structure of CB_1R binding with O-1860 after 100 ns. (D) Snapshot of the MD-simulated structure of CB_2R binding with O-1860 after 100 ns. (E) Decomposed per-residue binding energies for residues surrounding O-1860.

quantitatively validated through the combined MD and MM-PBSA binding free energy calculations (Table 1). Through the

https://dx.doi.org/10.1021/acschemneuro.0c00551
ACS Chem. Neurosci. XXXX, XXX, XXX−XXX

Table 1. Binding Free Energies (kcal/mol) of O-1860 with CB_1R and CB_2R Based on the Combined MD Simulation and MM-PBSA Calculations

CBRs	ΔE_{ele}	ΔE_{vdw}	ΔE_{gas}	ΔE_{pbsol}	ΔE_{pb}	$-T\Delta S$	ΔG_{PB}
CB_1R	−27.54	−70.34	−97.88	38.06	−59.82	22.04	−37.78
CB_2R	−16.37	−66.42	−82.79	39.75	−43.03	23.70	−19.33

Table 2. Calculated Binding Free Energies (Kcal/Mol) Compared to the Corresponding Experimental Binding Free Energies (kcal/mol, Derived from the Experimental K_i Shown in Figure 1 or 2)

	$\Delta G(CB_1R)$			$\Delta G(CB_2R)$			$\Delta G(CB_1R)$-$\Delta G(CB_2R)$	
ligand[a]	ΔG_{PB}[b]	ΔG_{corr}[c]	ΔG_{exp}[d]	ΔG_{PB}[b]	ΔG_{corr}[c]	ΔG_{exp}[d]	$\Delta\Delta G_{corr}$[c,e]	$\Delta\Delta G_{exp}$[f]
ACEA[52]	−39.07	−12.08	−12.15	−18.19	−7.60	−7.82	−4.98	−4.33
O-1860[27]	−38.44	−11.97	−11.88	−19.30	−7.96	−6.86	−4.54	−5.02
ACPA[53]	−36.78	−11.67	−11.88	−24.95	−9.79	−8.44	−2.68	−3.45
O-1812[27]	−35.54	−11.44	−11.62	−18.06	−7.56	−7.43	−4.12	−4.20
AM881[53]	−35.45	−11.43	−11.36	−26.78	−10.38	−9.64	−1.87	−1.72
AM883[54]	−35.10	−11.36	−10.99	−25.48	−9.96	−9.12	−2.11	−1.86
VJ-115[28]	−21.05	−8.82	−7.52	−25.19	−9.86	−8.60	1.39	1.08
R-methanandamide[53]	−29.66	−10.38	−10.57	−22.18	−8.89	−8.36	−1.57	−2.21
2-AG[53]	−29.28	−10.31	−9.93	−24.23	−9.55	−9.39	−0.95	−0.54
anandamide[53]	−27.69	−10.02	−9.90	−19.37	−7.98	−7.84	−1.79	−2.06
AM1174[55]	−25.09	−9.55	−9.53	−16.34	−7.00	−7.48	−1.89	−2.05
O-1811[27]	−24.13	−9.38	−9.52	−19.74	−8.10	−8.37	−0.79	−1.16
S-methanandamide[25]	−23.83	−9.32	−9.28	−19.40	−7.99	−6.98	−0.80	−2.30
PNR-4-20[28]	−25.79	−9.67	−9.33	−26.52	−10.29	−12.00	0.52	2.67
PNR-4-04[28]	−25.22	−9.57	−9.43	−25.84	−10.07	−10.89	0.49	1.46
PNR-4-02[28]	−27.64	−10.01	−9.80	−27.78	−10.70	−10.57	0.37	0.77
PNR-4-05[28]	−21.95	−8.98	−8.85	−24.10	−9.51	−9.83	0.88	0.98
PNR-4-99[28]	−25.28	−9.58	−9.54	−25.78	−10.06	−9.81	0.46	0.28
PNR-9−33[28]	−16.18	−7.93	−7.60	−23.26	−9.24	−9.55	2.13	1.95
PNR-4-03[28]	−28.42	−10.15	−9.63	−23.26	−9.24	−9.57	−0.98	−0.06
PNR-4-15[28]	−28.18	−10.11	−9.96	−20.72	−8.42	−9.53	−1.57	−0.43
PNR-4-17[28]	−16.52	−7.99	−8.26	−19.31	−7.96	−8.55	1.04	0.29
RMSD (kcal/mol)		**0.35**			**0.75**		**0.75**	

[a]The superscript after the ligand name refers to the reference for the experimental K_i (shown in Figure 1 or 2) used to derive the experimental binding free energy. [b]Calculated binding free energies obtained from the MM-PBSA calculations without any empirical correction. [c]Calculated binding free energies after empirical correction using eq 1−3. [d]The experimental binding free energy was converted from the experimental K_i using the well-known thermodynamic equation: $\Delta G_{exp} = -RT\ln(K_i)$. [e]$\Delta\Delta G_{corr}$ is the corrected binding free energy difference ($\Delta G(CB_1R) - \Delta G(CB_2R)$). [f]$\Delta\Delta G_{exp} = -RT\ln(K_i\ (CB_1R)/K_i(CB_2R)) = \Delta G_{exp}(CB_1R) - \Delta G_{exp}(CB_2R)$.

decomposition of the per-residue contributions to the binding energy, it was revealed that the residues 177, 267, 268, 279, 376, 379, and 380 within CB_1R had greater binding affinities with O-1860 (Figure 3D) than their corresponding analogues in CB_2R.

The Binding Mode of Long-Chain Molecules. To further verify our binding model, 12 additional long-chain molecules with known K_i values for the CB receptors were collected (Figure 1), and their binding free energies were estimated via the MD/MM-PBSA methodology. For each of the long-chain agonists examined in this study, according to the computational data (Table 2) the binding affinity is shown to be higher with the CB_1R over the CB_2R, this is consistent with previously obtained experimental data.[27,52−55] This selectivity for CB_1R extends to anandamide, which has previously been erroneously reported as a nonselective CB agonist.[56] However, these previous reports were performed in tissue-based assays, which contained amidohydrolases that degraded anandamide.[57−60] When these confounding enzymes are inhibited using phenylmethylsulfonyl fluoride (PMSF), the K_i of anandamide decreased considerably (543 nM against CB_1R w/o PMSF vs 90 nM against CB_1R w/PMSF), revealing its true selectivity for CB_1R over CB_2R (K_i = 1980 nM against CB_2R w/PMSF).[56,57] The computational results obtained have a high correlation with the experimental data, with R^2 of 0.8318 (Figure S2). When compared to O-1860, these long-chain endocannabinoids have similar per-residue contributions to their binding free energies, suggesting that these compounds bind similarly to O-1860 with the CB receptors. (Figure 3E)

Structure−Activity and Structure−Selectivity Correlation Relationships of Endocannabinoids. O-1860 represents the culmination of a series of additions to the endogenous cannabinoid anandamide, each step of which incrementally increases the binding affinity with CB_1R. The first change to O-1860 from anandamide involves the substitution of two additional methyl groups onto carbon-17, turning it into a neopentane moiety. These additional methyl groups allow for additional vdW interactions with the primarily hydrophobic pocket formed by TM4 and TM5 including F268 and W279 (Figure 3C). Additionally, the substitution of the terminal hydroxyl group with a halogen increases the favorable vdW interactions with the mainly hydrophobic pocket between TM3 and TM4 (Figure 3C) over the endocannabinoid (*R*)-methanandamide (Figure 4A). The second modification of

https://dx.doi.org/10.1021/acschemneuro.0c00551
ACS Chem. Neurosci. XXXX, XXX, XXX−XXX

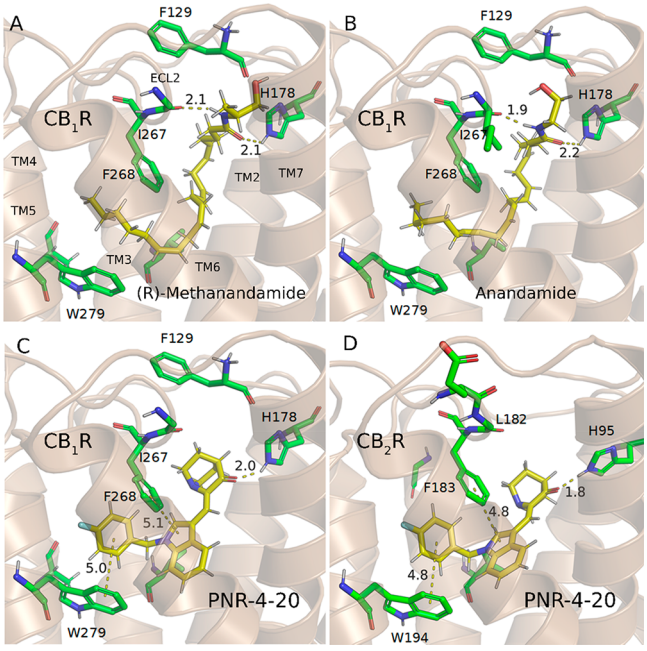

Figure 4. Binding modes of representative long-chain compounds in CB_1R and CB_2R. (A) CB_1R binding with (*R*)-methanandamide. (B) CB_1R binding with anandamide. The binding mode of O-1860 with CB_1R consists of two hydrogen bonds with H178 and I267. Additionally, favorable hydrophobic interactions are created with F268 and W279. The removal of the neo-pentane and bromide on the long aliphatic chain further reduces the binding affinity with the CB_1R receptor for (*R*)-methanandamide. The removal of the methyl group adjacent to the amide headgroup further removes the selectivity and potency to the original endocannabinoid anandamide. (C) Binding pose of PNR-4-20 with CB_1R. (D) Binding pose of PNR-4-20 with CB_2R. PNR-4-20 binds within the central binding pocket of the receptors, surrounded by several hydrophobic residues including F268 and W279 in CB_1R and F183 and W194 in CB_2R. The carbonyl formed hydrogen bond with His178/95 of CB_1R/CB_2R. A slight rotation in the central indole ring is the only major difference between these two binding poses, demonstrating the similarity in the binding pockets between the two receptors.

anandamide (Figure 4B) comes from an additional methyl group placed one carbon from the terminal hydroxyl group (Figure 4A) allowing for additional vdW interactions with I267.

The Binding Mode of the IQD Series of Compounds. Furthermore, we used the IQD derivatives shown in Figure 2 to test our models. It is gratifying that the calculated results were in good agreement to the experimental data, suggesting that these models also can be used to the drug design for this series of compounds. Key to the binding of these compounds to each receptor is the carbonyl group on the quinuclidine ring accepting a hydrogen bond from the nearby H178/95 residue in CB_1R/CB_2R. Additionally, these compounds have strong hydrophobic interactions in both CB_1R and CB_2R with nearby F268 and W279 in CB_1R (F183 and W194in CB_2R) (Figures S15−S22). PNR-4-20 (Figure 4C and D) represents both a G-protein biased and potent CB_1R agonist, only lacking in selectivity for one of the receptors (or limited selectivity for CB_2R). This lack in selectivity for CB_1R is readily apparent when one looks at the binding mode comparison (Figure 4C and D) where the only major change in position is a slight rotation in the central indole ring. The similarity of the central binding pocket for the CB receptors is the main hindrance toward developing selective CB receptor agonists. The binding poses proposed for the endocannabinoids and their analogues, shown in the above, give clues as to how these compounds could be modified to allow for CBreceptor selectivity.

The Correction of Binding Free Energies. Summarized in Table 2 are the binding free energies obtained from the MM-PBSA calculations in comparison with the corresponding binding free energies for CB_1R and CB_2R with all of the 23 ligands shown in Figure 1 and 2. As seen in Table 2, our computational protocol performs similarly well with both the long-chain cannabinoids and the typical IQD derivatives. The relative magnitudes of the MM-PBSA binding free energy (ΔG_{PB}) values are qualitatively consistent with the relative experimental binding free energies in terms of the structure−activity relationship (SAR) for each receptor and the receptor selectivity between CB_1R and CB_2R (Figure 5).

In terms of the absolute binding free energies, it is not surprising to note that the MM-PBSA calculations systematically overestimated the binding affinities of the ligands with both CB_1R and CB_2R. Nevertheless, the empirical linear correlation relationships indicated in Figure 5 may be used to empirically correct the calculated binding free energies. Particularly, for CB_1R binding with ligands, we have

$$\Delta G_{corr}(CB_1R) = 0.1939\Delta G_{PB}(CB_1R) - 4.5021 \quad (1)$$

with a correlation coefficient (R^2) of 0.9381 and RMSD of 0.36 kcal/mol. For CB_2R binding with ligands, we have

$$\Delta G_{corr}(CB_2R) = 0.3057\Delta G_{PB}(CB_2R) - 2.0485 \quad (2)$$

with $R^2 = 0.6334$ and RMSD = 0.75 kcal/mol. In addition, for the difference in the binding free energy between CB_1R and CB_2R, we have

$$\Delta\Delta G_{corr} = 0.2619\Delta\Delta G_{PB} + 0.4457 \quad (3)$$

with $R^2 = 0.8649$ and RMSD = 0.69 kcal/mol. In eq 3, $\Delta\Delta G_{PB} = \Delta G_{PB}(CB_1R) - \Delta G_{PB}(CB_2R)$ and $\Delta\Delta G_{corr}$ is the corrected binding free energy difference reflecting the selectivity between CB_1R and CB_2R. In all of these equations, ΔG_{PB} represents the binding free energy obtained directly from the MM-PBSA calculation, whereas ΔG_{corr} refers to the corrected binding free energy.

As seen in Table 2, the empirically corrected binding free energies with both CB_1R and CB_2R, as well as the difference between them, are all in excellent agreement with the corresponding experimental data, suggesting that the binding modes determined in this study are reasonable. Furthermore, our models are expected to be valuable for the rational drug design in the future.

In summary, using molecular docking, MD simulation, and MM-PBSA binding free energy calculations, we have been able to determine the binding modes of CB_1R and CB_2R interacting with both the IQD series of ligands and long-chain cannabinoids (including their synthetic analogues). Based on the obtained binding poses, the calculated relative binding free energies are in good agreement with the corresponding experimental binding affinity data in terms of the SAR for each receptor (CB_1R or CB_2R) and the receptor selectivity between CB_1R and CB_2R. The binding poses for the long-chain cannabinoids and their synthetic analogues implicate the site surrounded by the TM2, TM7, and ECL-2 regions as being vital for providing the long-chain ligands with the selectivity for CB_1R, especially the I267/L182 of CB_1R/CB_2R. Considering this computational insight, the future rational

https://dx.doi.org/10.1021/acschemneuro.0c00551
ACS Chem. Neurosci. XXXX, XXX, XXX−XXX

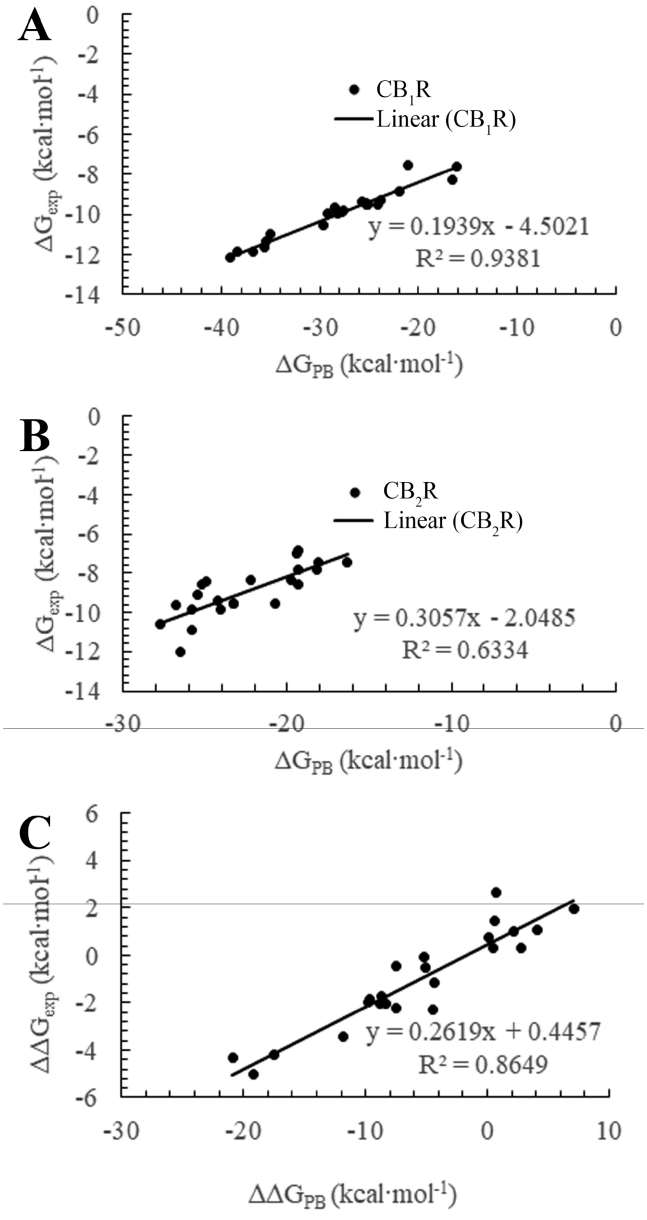

Figure 5. (A) Calculated binding free energy vs experimental binding free energy of ligands with CB_1R. (B) Calculated binding free energy vs experimental binding free energy of ligands with CB_2R. (C) Difference in experimental binding free energy vs the calculated binding free energy difference between CB_1R and CB_2R. These measures indicate that there is a strong correlation between the difference in the calculated and experimental binding free energy, allowing us to successfully predict the selectivity for a given ligand toward CB_1R or CB_2R as well as determine their relative affinity.

design of new selective ligands for CB_1R and CB_2R may be focused on favorable interactions with this site. Particularly, as we have also determined the binding poses of the IQD compounds including the unique G-protein biased agonist PNR-4-20 and PNR-4-02, new compounds may be designed that bring the features of both classes of molecules together, creating selective, potent, and G-protein biased IQD/endocannabinoid hybrids. The similar computational strategy used in this study may also prove fruitful in applications with other GCPRs or membrane-bound proteins.

METHODS

Multiple Sequences Alignment. The amino-acid sequences of CB_1R and CB_2R were downloaded from the Uniprot database.[61] The multiple sequence alignment was performed using the MUSCLE software, which also was used to calculate sequence identity.[62] The figure for sequence alignment was generated using the ESPript 3.0 software.[63]

Docking and Molecular Dynamics Simulations. The cannabinoid receptors (PDB ID: 5XRA for CB_1R and 6PT0 for CB_2R) were prepared using the PDB 2PQR module to fix any potential errors with the models and to additionally assign the ff14SB force field parameters to the constituent atoms.[22,35] The structures of ligands were built and energy-minimized using the SYBYL v2.0 software (Tripos Inc., St. Louis, MO). Initial poses for the ligands were predicted using the AutoDock 4.2 software with the default parameters.[64] To improve the efficiency of calculation, the CB_2R model was superimposed to the CB_1R model. The grid size was set to 60 × 60 × 60, and the grid center was designated at −43.616, 164.787, 306.920. For each ligand, 265 possible binding poses were generated for further study. Each ligand had its atomic charges calculated through the AM1-BCC method in the Antechamber module and was subsequently energy-minimized through the Sander module of AMBER16 program before being placed within the binding site of each receptor.[65−67]

For the compound O-1860 binding with each receptor, the complexes were inserted into a POPC lipid bilayer through the use of the Membrane-Builder module of CHARMM-GUI.[68] Then the complex structures were energy-minimized over five steps: an initial energy minimization where only hydrogens and lipid bilayer were energy-minimized, followed by energy minimization of the ligand, receptor hydrogens, and lipid bilayer, followed by side chains of the receptor, residues within 6 Å of the ligand, and finally the entire system. Each of these steps consisted of a total of 3000 energy minimization steps. Then the MD simulation of the energy-minimized complex was performed using the CUDA accelerated PMEMD module of AMBER.[65] After energy minimization and heating of the lipid/complex system, 100 ns of MD simulations were performed. One hundred snapshots of the last nanosecond of the system were used within the MM-PBSA module of the AMBER to make sure that the binding free energy based on the final snapshot is reasonably close to the average of binding free energies associated with the one hundred snapshots. The energy decomposition was performed using the decomposition option within the MMPBSA module of the AMBER16.

The last snapshot of the MD-simulated complex with O-1860 was subsequently used as the receptor with O-1860 and lipid bilayer removed. Each ligand (including O-1860) was then placed into the receptor based on the previously obtained binding poses from the AutoDock software.[64] The whole complex structure was then energy-minimized, and had its binding free energy calculated using the same MM-PBSA methodology.

ASSOCIATED CONTENT

Supporting Information

Additional figures for the . The Supporting Information is available free of charge at https://pubs.acs.org/doi/10.1021/acschemneuro.0c00551.

Sequence alignment of human, mouse, and rat CB receptors, correction of MM-PBSA binding free energies with the corresponding experimental binding free energies for the long-chain ligands, and modeled binding structures of CB_1R and CB_2R with various ligands (PDF)

https://dx.doi.org/10.1021/acschemneuro.0c00551
ACS Chem. Neurosci. XXXX, XXX, XXX−XXX

AUTHOR INFORMATION

Corresponding Author

Chang-Guo Zhan − *Molecular Modeling and Biopharmaceutical Center and Department of Pharmaceutical Sciences, College of Pharmacy, University of Kentucky, Lexington, Kentucky 40536, United States;* orcid.org/0000-0002-4128-7269; Phone: 859-323-3943; Email: zhan@uky.edu; Fax: 859-257-7585

Authors

Jing-Fang Yang − *Molecular Modeling and Biopharmaceutical Center and Department of Pharmaceutical Sciences, College of Pharmacy, University of Kentucky, Lexington, Kentucky 40536, United States*

Alexander H. Williams − *Molecular Modeling and Biopharmaceutical Center and Department of Pharmaceutical Sciences, College of Pharmacy, University of Kentucky, Lexington, Kentucky 40536, United States*

Narsimha R. Penthala − *Department of Pharmaceutical Sciences, College of Pharmacy, University of Arkansas for Medical Sciences, Little Rock, Arkansas 72205, United States*

Paul L. Prather − *Department of Pharmacology and Toxicology, College of Medicine, University of Arkansas for Medical Sciences, Little Rock, Arkansas 72205, United States*

Peter A. Crooks − *Department of Pharmaceutical Sciences, College of Pharmacy, University of Arkansas for Medical Sciences, Little Rock, Arkansas 72205, United States*

Complete contact information is available at: https://pubs.acs.org/10.1021/acschemneuro.0c00551

Author Contributions

J.-F.Y. and A.H.W. contributed equally to this work. J.-F.Y. and A.H.W. performed computational experiments, analyzed the data, and drafted the manuscript. N.R.P., P.LP., and P.A.C. analyzed the data. C.-G.Z. designed the computational experiments, analyzed the data, and finalized the manuscript.

Notes

The authors declare no competing financial interest.

ACKNOWLEDGMENTS

This work was supported in part by the funding of the Molecular Modeling and Biopharmaceutical Center at the University of Kentucky College of Pharmacy, the National Science Foundation (NSF Grant CHE-1111761), and the National Institutes of Health (P20 GM130456, UL1TR001998, T32 DA016176, and R01DA039143). The authors also acknowledge the Computer Center at University of Kentucky for supercomputing time on a Dell Supercomputer Cluster consisting of 388 nodes or 4816 processors.

REFERENCES

(1) Hauser, A. S., Attwood, M. M., Rask-Andersen, M., Schiöth, H. B., and Gloriam, D. E. (2017) Trends in GPCR Drug Discovery: New Agents, Targets and Indications. *Nat. Rev. Drug Discovery 16* (12), 829−842.

(2) Basu, S., and Dittel, B. N. (2011) Unraveling the Complexities of Cannabinoid Receptor 2 (CB2) Immune Regulation in Health and Disease. *Immunol. Res. 51* (1), 26−38.

(3) Baron, E. P., Lucas, P., Eades, J., and Hogue, O. (2018) Patterns of Medicinal Cannabis Use, Strain Analysis, and Substitution Effect among Patients with Migraine, Headache, Arthritis, and Chronic Pain in a Medicinal Cannabis Cohort. *J. Headache Pain 19* (1), 37.

(4) Vučković, S., Srebro, D., Vujović, K. S., Vučetić, Č., and Prostran, M. (2018) Cannabinoids and Pain: New Insights from Old Molecules. *Front. Pharmacol. 9*, 1259.

(5) Abrams, D. I., Couey, P., Shade, S. B., Kelly, M. E., and Benowitz, N. L. (2011) Cannabinoid-Opioid Interaction in Chronic Pain. *Clin. Pharmacol. Ther. 90* (6), 844−851.

(6) Cichewicz, D. L., and McCarthy, E. A. (2003) Antinociceptive Synergy between Delta(9)-Tetrahydrocannabinol and Opioids after Oral Administration. *J. Pharmacol. Exp. Ther. 304* (3), 1010−1015.

(7) Lötsch, J., Weyer-Menkhoff, I., and Tegeder, I. (2018) Current Evidence of Cannabinoid-Based Analgesia Obtained in Preclinical and Human Experimental Settings. *Eur. J. Pain 22* (3), 471−484.

(8) Benedetti, F., Amanzio, M., Rosato, R., and Blanchard, C. (2011) Nonopioid Placebo Analgesia Is Mediated by CB1 Cannabinoid Receptors. *Nat. Med. 17* (10), 1228−1230.

(9) Agarwal, N., Pacher, P., Tegeder, I., Amaya, F., Constantin, C. E., Brenner, G. J., Rubino, T., Michalski, C. W., Marsicano, G., Monory, K., et al. (2007) Cannabinoids Mediate Analgesia Largely Via Peripheral Type 1 Cannabinoid Receptors in Nociceptors. *Nat. Neurosci. 10* (7), 870−879.

(10) Burns, T. L., and Ineck, J. R. (2006) Cannabinoid Analgesia as a Potential New Therapeutic Option in the Treatment of Chronic Pain. *Ann. Pharmacother. 40* (2), 251−260.

(11) Walker, J. M., and Huang, S. M. (2002) Cannabinoid Analgesia. *Pharmacol. Ther. 95* (2), 127−135.

(12) Abdallah, F. W., Hussain, N., Weaver, T., and Brull, R. (2020) Analgesic Efficacy of Cannabinoids for Acute Pain Management after Surgery: A Systematic Review and Meta-Analysis. *Reg. Anesth. Pain Med. 45* (7), 509−519.

(13) Wiese, B., and Wilson-Poe, A. R. (2018) Emerging Evidence for Cannabis' Role in Opioid Use Disorder. *Cannabis Cannabinoid Res. 3* (1), 179−189.

(14) Rice, A. (2001) Cannabinoids and Pain. *Curr. Opin. Invest. Drugs 2* (3), 399.

(15) Rossi, F., Punzo, F., Umano, G. R., Argenziano, M., and Miraglia Del Giudice, E. (2018) Role of Cannabinoids in Obesity. *Int. J. Mol. Sci. 19* (9), 2690.

(16) Pertwee, R. G. (2012) Targeting the Endocannabinoid System with Cannabinoid Receptor Agonists: Pharmacological Strategies and Therapeutic Possibilities. *Philos. Trans. R. Soc., B 367* (1607), 3353−3363.

(17) Pertwee, R. G. (2009) Emerging Strategies for Exploiting Cannabinoid Receptor Agonists as Medicines. *Br. J. Pharmacol. 156* (3), 397−411.

(18) Shahbazi, F., Grandi, V., Banerjee, A., and Trant, J. F. (2020) Cannabinoids and Cannabinoid Receptors: The Story So Far. *iScience 23*, 101301.

(19) Song, Z.-H., Slowey, C.-A., Hurst, D. P., and Reggio, P. H. (1999) The Difference between the CB1 and CB2cannabinoid Receptors at Position 5.46 Is Crucial for the Selectivity of WIN55212-2 for CB2. *Mol. Pharmacol. 56* (4), 834−840.

(20) Tuccinardi, T., Ferrarini, P. L., Manera, C., Ortore, G., Saccomanni, G., and Martinelli, A. (2006) Cannabinoid CB2/CB1 Selectivity. Receptor Modeling and Automated Docking Analysis. *J. Med. Chem. 49* (3), 984−994.

(21) Hua, T., Vemuri, K., Nikas, S. P., Laprairie, R. B., Wu, Y., Qu, L., Pu, M., Korde, A., Jiang, S., Ho, J.-H., et al. (2017) Crystal Structures of Agonist-Bound Human Cannabinoid Receptor CB1. *Nature 547* (7664), 468−471.

(22) Hua, T., Vemuri, K., Pu, M., Qu, L., Han, G. W., Wu, Y., Zhao, S., Shui, W., Li, S., Korde, A., et al. (2016) Crystal Structure of the Human Cannabinoid Receptor CB1. *Cell 167* (3), 750−762.

(23) Herzberg, U., Eliav, E., Bennett, G., and Kopin, I. J. (1997) The Analgesic Effects of R (+)-Win 55,212−2 Mesylate, a High Affinity Cannabinoid Agonist, in a Rat Model of Neuropathic Pain. *Neurosci. Lett. 221* (2−3), 157−160.

(24) Diaz, P., Phatak, S. S., Xu, J., Astruc-Diaz, F., Cavasotto, C. N., and Naguib, M. (2009) 6-Methoxy-N-Alkyl Isatin Acylhydrazone Derivatives as a Novel Series of Potent Selective Cannabinoid

Receptor 2 Inverse Agonists: Design, Synthesis, and Binding Mode Prediction. *J. Med. Chem. 52* (2), 433−444.
(25) Vemuri, V. K., and Makriyannis, A. (2009) Endocannabinoids and Their Synthetic Analogs. In *The Cannabinoid Receptors*, pp 21−48, Springer.
(26) Pertwee, R. G., Howlett, A. C., Abood, M. E., Alexander, S. P. H., Di Marzo, V., Elphick, M. R., Greasley, P. J., Hansen, H. S., Kunos, G., Mackie, K., Mechoulam, R., and Ross, R. A. (2010) International Union of Basic and Clinical Pharmacology. Lxxix. Cannabinoid Receptors and Their Ligands: Beyond CB1 and CB2. *Pharmacol. Rev. 62*, 588−631.
(27) Di Marzo, V., Bisogno, T., De Petrocellis, L., Brandi, I., Jefferson, R.G., Winckler, R.L., Davis, J.B., Dasse, O., Mahadevan, A., Razdan, R.K., and Martin, B.R. (2001) Highly Selective CB1 Cannabinoid Receptor Ligands and Novel CB1/Vr1 Vanilloid Receptor "Hybrid" Ligands. *Biochem. Biophys. Res. Commun. 281* (2), 444−451.
(28) Madadi, N. R., Penthala, N. R., Brents, L. K., Ford, B. M., Prather, P. L., and Crooks, P. A. (2013) Evaluation of (Z)-2-((1-Benzyl-1h-Indol-3-Yl)Methylene)-Quinuclidin-3-One Analogues as Novel, High Affinity Ligands for CB1 and CB2 Cannabinoid Receptors. *Bioorg. Med. Chem. Lett. 23* (7), 2019−2021.
(29) Ford, B. M., Franks, L. N., Tai, S., Fantegrossi, W. E., Stahl, E. L., Berquist, M. D., Cabanlong, C. V., Wilson, C. D., Penthala, N. R., Crooks, P. A., and Prather, P. L. (2017) Characterization of Structurally Novel G Protein Biased CB1 Agonists: Implications for Drug Development. *Pharmacol. Res. 125*, 161−177.
(30) Kendall, D., Alexander, S., Priestley, R., Asghar, M., and von Mentzer, B. (2017) Biased Agonism at Cannabinoid CB1 and Δ-Opioid Receptors; Therapeutic Potential. *Neuropeptides 65*, 131.
(31) Newman-Tancredi, A. (2011) Biased Agonism at Serotonin 5-Ht1a Receptors: Preferential Postsynaptic Activity for Improved Therapy of Cns Disorders. *Neuropsychiatry 1* (2), 149.
(32) Rankovic, Z., Brust, T. F., and Bohn, L. M. (2016) Biased Agonism: An Emerging Paradigm in Gpcr Drug Discovery. *Bioorg. Med. Chem. Lett. 26* (2), 241−250.
(33) Whalen, E. J., Rajagopal, S., and Lefkowitz, R. J. (2011) Therapeutic Potential of B-Arrestin-and G Protein-Biased Agonists. *Trends Mol. Med. 17* (3), 126−139.
(34) Hua, T., Li, X., Wu, L., Iliopoulos-Tsoutsouvas, C., Wang, Y., Wu, M., Shen, L., Johnston, C. A., Nikas, S. P., Song, F., et al. (2020) Activation and Signaling Mechanism Revealed by Cannabinoid Receptor-Gi Complex Structures. *Cell 180* (4), 655−665.
(35) Xing, C., Zhuang, Y., Xu, T.-H., Feng, Z., Zhou, X. E., Chen, M., Wang, L., Meng, X., Xue, Y., Wang, J., et al. (2020) Cryo-Em Structure of the Human Cannabinoid Receptor CB2-Gi Signaling Complex. *Cell 180* (4), 645−654.
(36) Li, X., Hua, T., Vemuri, K., Ho, J.-H., Wu, Y., Wu, L., Popov, P., Benchama, O., Zvonok, N., Qu, L., et al. (2019) Crystal Structure of the Human Cannabinoid Receptor CB2. *Cell 176* (3), 459−467.
(37) Salo, O. M., Lahtela-Kakkonen, M., Gynther, J., Järvinen, T., and Poso, A. (2004) Development of a 3d Model for the Human Cannabinoid CB1 Receptor. *J. Med. Chem. 47* (12), 3048−3057.
(38) Sapundzhi, F., and Dzimbova, T. (2020) A Computational Study of Cannabinoid Receptors and Cannabinoid Ligands. *J. Chem. Technol. Metall. 55* (5), 959−964.
(39) Reggio, P. H., and Traore, H. (2000) Conformational Requirements for Endocannabinoid Interaction with the Cannabinoid Receptors, the Anandamide Transporter and Fatty Acid Amidohydrolase. *Chem. Phys. Lipids 108* (1−2), 15−35.
(40) Lynch, D. L., and Reggio, P. H. (2005) Molecular Dynamics Simulations of the Endocannabinoid N-Arachidonoylethanolamine (Anandamide) in a Phospholipid Bilayer: Probing Structure and Dynamics. *J. Med. Chem. 48* (15), 4824−4833.
(41) Reggio, P. H. (2010) Endocannabinoid Binding to the Cannabinoid Receptors: What Is Known and What Remains Unknown. *Curr. Med. Chem. 17* (14), 1468−1486.
(42) Lin, S., Khanolkar, A. D., Fan, P., Goutopoulos, A., Qin, C., Papahadjis, D., and Makriyannis, A. (1998) Novel Analogues of Arachidonylethanolamide (Anandamide): Affinities for the CB1 and CB2 Cannabinoid Receptors and Metabolic Stability. *J. Med. Chem. 41* (27), 5353−61.
(43) Dainese, E., Gasperi, V., and Maccarrone, M. (2005) Partial Qsar Analysis of Some Selected Natural Inhibitors of Faah Suggests a Working Hypothesis for the Development of Endocannabinoid-Based Drugs. *Curr. Drug Targets: CNS Neurol. Disord. 4* (6), 709−714.
(44) McAllister, S. D., Rizvi, G., Anavi-Goffer, S., Hurst, D. P., Barnett-Norris, J., Lynch, D. L., Reggio, P. H., and Abood, M. E. (2003) An Aromatic Microdomain at the Cannabinoid CB1 Receptor Constitutes an Agonist/Inverse Agonist Binding Region. *J. Med. Chem. 46* (24), 5139−5152.
(45) Perez, A., Morrone, J. A., Simmerling, C., and Dill, K. A. (2016) Advances in Free-Energy-Based Simulations of Protein Folding and Ligand Binding. *Curr. Opin. Struct. Biol. 36*, 25−31.
(46) Loo, J. S., Yong, A. Y., and Yong, Y. N. (2020) The Effect of Multiple Simulation Parameters on MM/PBSA Performance for Binding Affinity Prediction of CB1 Cannabinoid Receptor Agonists and Antagonists. *Chem. Biol. Drug Des.*, DOI: 10.1111/cbdd.13733.
(47) Huang, X., Zheng, F., and Zhan, C.-G. (2008) Modeling Differential Binding of A4β2 Nicotinic Acetylcholine Receptor with Agonists and Antagonists. *J. Am. Chem. Soc. 130* (49), 16691−16696.
(48) Huang, X., Zheng, F., Chen, X., Crooks, P. A., Dwoskin, L. P., and Zhan, C.-G. (2006) Modeling Subtype-Selective Agonists Binding with A4β2 and A7 Nicotinic Acetylcholine Receptors: Effects of Local Binding and Long-Range Electrostatic Interactions. *J. Med. Chem. 49* (26), 7661−7674.
(49) Huang, X., Zheng, F., Crooks, P. A., Dwoskin, L. P., and Zhan, C.-G. (2005) Modeling Multiple Species of Nicotine and Deschloroepibatidine Interacting with A4β2 Nicotinic Acetylcholine Receptor: From Microscopic Binding to Phenomenological Binding Affinity. *J. Am. Chem. Soc. 127* (41), 14401−14414.
(50) Jin, Y., Huang, X., Papke, R. L., Jutkiewicz, E. M., Showalter, H. D., and Zhan, C.-G. (2017) Design, Synthesis, and Biological Activity of 5′-Phenyl-1, 2, 5, 6-Tetrahydro-3, 3′-Bipyridine Analogues as Potential Antagonists of Nicotinic Acetylcholine Receptors. *Bioorg. Med. Chem. Lett. 27* (18), 4350−4353.
(51) Huang, X., Zheng, F., Stokes, C., Papke, R. L., and Zhan, C.-G. (2008) Modeling Binding Modes of A7 Nicotinic Acetylcholine Receptor with Ligands: The Roles of Gln117 and Other Residues of the Receptor in Agonist Binding. *J. Med. Chem. 51* (20), 6293−6302.
(52) Hillard, C. J., Manna, S., Greenberg, M. J., DiCamelli, R., Ross, R. A., Stevenson, L. A., Murphy, V., Pertwee, R. G., and Campbell, W. B. (1999) Synthesis and Characterization of Potent and Selective Agonists of the Neuronal Cannabinoid Receptor (CB1). *J. Pharmacol. Exp. Ther. 289* (3), 1427−1433.
(53) Thakur, G. A., Nikas, S. P., and Makriyannis, A. (2005) CB1 Cannabinoid Receptor Ligands. *Mini-Rev. Med. Chem. 5* (7), 631−640.
(54) Willinsky, M. (2018) Composition and Methods to Improve Stability, Dosing, Pharmacodynamics and Product Shelf Life of Endocannabinoids, Phytocannabinoids and Synthetic Cannabinoids Delivered by Nasal Inhaler. US 20180000727A1.
(55) Lin, S., Khanolkar, A. D., Fan, P., Goutopoulos, A., Qin, C., Papahadjis, D., and Makriyannis, A. (1998) Novel Analogues of Arachidonylethanolamide (Anandamide): Affinities for the CB1 and CB2 Cannabinoid Receptors and Metabolic Stability. *J. Med. Chem. 41* (27), 5353−5361.
(56) Felder, C. C., Joyce, K. E., Briley, E. M., Mansouri, J., Mackie, K., Blond, O., Lai, Y., Ma, A. L., and Mitchell, R. L. (1995) Comparison of the Pharmacology and Signal Transduction of the Human Cannabinoid CB1 and CB2 Receptors. *Mol. Pharmacol. 48* (3), 443−450.
(57) Adams, I. B., Ryan, W., Singer, M., Thomas, B. F., Compton, D. R., Razdan, R. K., and Martin, B. R. (1995) Evaluation of Cannabinoid Receptor Binding and in Vivo Activities for Anandamide Analogs. *J. Pharmacol. Exp. Ther. 273* (3), 1172−1181.
(58) Wiley, J. L., Dewey, M. A., Jefferson, R. G., Winckler, R. L., Bridgen, D. T., Willoughby, K. A., and Martin, B. R. (2000) Influence

of Phenylmethylsulfonyl Fluoride on Anandamide Brain Levels and Pharmacological Effects. *Life Sci. 67* (13), 1573−1583.
(59) Compton, D. R., and Martin, B. R. (1997) The Effect of the Enzyme Inhibitor Phenylmethylsulfonyl Fluoride on the Pharmacological Effect of Anandamide in the Mouse Model of Cannabimimetic Activity. *J. Pharmacol. Exp. Ther. 283* (3), 1138−1143.
(60) Laine, K., Järvinen, K., Pate, D. W., Urtti, A., and Järvinen, T. (2002) Effect of the Enzyme Inhibitor, Phenylmethylsulfonyl Fluoride, on the Iop Profiles of Topical Anandamides. *Invest. Ophthalmol. Vis. Sci. 43* (2), 393−397.
(61) The UniProt Consortium (2008) The Universal Protein Resource (Uniprot). *Nucleic Acids Res. 36*, D190−D195.
(62) Edgar, R. C. (2004) Muscle: Multiple Sequence Alignment with High Accuracy and High Throughput. *Nucleic Acids Res. 32* (5), 1792−1797.
(63) Robert, X., and Gouet, P. (2014) Deciphering Key Features in Protein Structures with the New Endscript Server. *Nucleic Acids Res. 42* (W1), W320−W324.
(64) Morris, G. M., Huey, R., Lindstrom, W., Sanner, M. F., Belew, R. K., Goodsell, D. S., and Olson, A. J. (2009) Autodock4 and Autodocktools4: Automated Docking with Selective Receptor Flexibility. *J. Comput. Chem. 30* (16), 2785−2791.
(65) Pearlman, D. A., Case, D. A., Caldwell, J. W., Ross, W. S., Cheatham, T. E., III, DeBolt, S., Ferguson, D., Seibel, G., and Kollman, P. (1995) Amber, a Package of Computer Programs for Applying Molecular Mechanics, Normal Mode Analysis, Molecular Dynamics and Free Energy Calculations to Simulate the Structural and Energetic Properties of Molecules. *Comput. Phys. Commun. 91* (1−3), 1−41.
(66) Jakalian, A., Jack, D. B., and Bayly, C. I. (2002) Fast, Efficient Generation of High-Quality Atomic Charges. Am1-Bcc Model: II. Parameterization and Validation. *J. Comput. Chem. 23* (16), 1623−41.
(67) Case, D. A., Cheatham, T. E., 3rd, Darden, T., Gohlke, H., Luo, R., Merz, K. M., Jr., Onufriev, A., Simmerling, C., Wang, B., and Woods, R. J. (2005) The Amber Biomolecular Simulation Programs. *J. Comput. Chem. 26* (16), 1668−88.
(68) Jo, S., Kim, T., Iyer, V. G., and Im, W. (2008) CHARMM-GUI: A Web-Based Graphical User Interface for Charmm. *J. Comput. Chem. 29* (11), 1859−1865.

https://dx.doi.org/10.1021/acschemneuro.0c00551
ACS Chem. Neurosci. XXXX, XXX, XXX−XXX